

2016-10

Optimal Power Dispatch in a Microgrid

Loza-López, Martín J.; Ruiz-Cruz, Riemann; López-García, Tania B.; Sanchez, Edgar; Sánchez-Torres, Juan D.

Loza-Lopez, M.J.; Ruiz-Cruz, R.; López-García, T. B.; Sánchez, E.N. and Sánchez-Torres, J.D. (2016) Optimal Power Dispatch in a Microgrid. Conference proceedings of the XVII Latin American Conference of Automatic Control, Medellín, Colombia, pp. 455--460.

Enlace directo al documento: <http://hdl.handle.net/11117/4289>

Este documento obtenido del Repositorio Institucional del Instituto Tecnológico y de Estudios Superiores de Occidente se pone a disposición general bajo los términos y condiciones de la siguiente licencia:
<http://quijote.biblio.iteso.mx/licencias/CC-BY-NC-2.5-MX.pdf>

(El documento empieza en la siguiente página)

Optimal Power Dispatch in a Microgrid

Martin J. Loza-Lopez * Riemann Ruiz-Cruz **
T.B. Lopez-Garcia * Edgar N. Sanchez *
Juan Diego Sánchez-Torres **

* Centro de Investigación y Estudios Avanzados del IPN, Zapopan, Jalisco, México, (e-mail: {mdloza,tblopez,sanchez}@gdl.cinvestav.mx)

** ITESO University, Periferico Sur Gomez Morin 8585, Tlaquepaque, Jalisco, México C.P. 45604, (e-mail: {riemannruiz,dsanchez}@iteso.mx)

Abstract: This paper is concerned with the power dispatch in a microgrid. The dispatch problem is formulated as linear program. Thus, the proposed solution is the application of neural network that solves linear programming on-line. This proposal is motivated by the increasing electric energy demand and the rising need to incorporate sustainable energy sources to the power grid in a reliable scheme. A microgrid is an interconnection of distributed energy sources (DES), with the tendency to include renewable energies that offer many advantages to customers and utilities. The different DES that compose the microgrid are controlled independently to track the optimal reference provided by the proposed method in order to supply a demanded power output minimizing the consumed power from the main grid.

Keywords: Electric energy distribution, Neurodynamic optimization, Linear programming, Power management

1. INTRODUCTION

The optimization of the power dispatch within a microgrid is a big challenge for many engineering areas as control, power electronics and modeling. Different studies have been performed in this area, some examples are presented in Chowdhury and Crossley (2009). In the presented work, the optimal amount of power to be supplied by each energy source in a microgrid simulation, to produce a maximum amount of energy, is analyzed. Because of the varying output power that renewable energy sources present, large-scale, real-time optimization procedures are required, most of them in the form of linear programming. In contrast to the publications which use recurrent neural networks for microgrid optimization (Aquino et al., 2010), the proposed approach provides *fixed convergence time* to the solution and the tuning of only one network parameter.

The optimization problem is stated to maximize or minimize an objective function with the manipulation of the value of decision variables, sometimes, subject to equality and/or inequality constraints. These problems typically require large-scale real-time linear programming procedures. Most of the time, sequential algorithms as the classical simplex or the interior point methods are implemented. However, these approaches have the disadvantage that the computing time required for a solution is greatly dependent on the problem dimension and structure.

Dynamical systems which can solve real-time optimization were introduced in Pyne (1956). Since then, other major contributions have been proposed by Korovin and Utkin (1974), Pazos and Bhaya (2009), Wang (1993) and Wilson (1986). Due to its inherent massive parallelism, these

systems are able to solve optimization problems faster than those using more popular optimization algorithms executed on general-purpose digital computers (Cichocki and Unbehauen, 1993), with great flexibility to parametric variations (Pyne, 1956).

Although the previous studies exhibit high performance, it is necessary to tune several network parameters, that increase linearly with the optimization problem dimension, since for every decision variable there is an individual selection of each activation function. In addition, the fixed time characteristic is not presented in most of the mentioned references.

In this paper, a dynamical system for the solution of linear programming in a predefined convergence time is proposed. Its design is considered as a sliding mode control problem, where the network structure is based on the Karush-Kuhn-Tucker (KKT) optimality conditions (Karush, 1939; Kuhn and Tucker, 1951) and the KKT multipliers are regarded as control inputs. The problem is solved without the individual selection of each stabilizing input, instead, a multivariable function based on the unit control (Utkin, 1992) is used. On the other hand, the fixed time stability (Polyakov, 2012) property ensures system convergence time independent of the initial conditions. This controller is used in the KKT multiplier design, enforcing a sliding mode in which the optimization problem is solved.

The proposed approach has attractive features such as: fixed time convergence to the optimization problem solution and a fixed number of parameters (one in this case), regardless of the optimization problem dimension. Therefore, it offers the scalability characteristic, that

allows the possibility of adding other energy sources to the microgrid.

In the following, Section 2 presents the mathematical preliminaries and some useful definitions. In Section 3 the basis of the linear programming problem are established and the proposed algorithm is presented. Section 4 describes the microgrid connection and the controllers implemented along with the linear programming problem for the power dispatch and shows the simulation results. Finally, in Section 5 the conclusions are presented.

2. MATHEMATICAL PRELIMINARIES

Consider the system

$$\dot{\xi} = f(t, \xi) \quad (1)$$

where $\xi \in \mathbb{R}^n$ and $f : \mathbb{R}_+ \times \mathbb{R}^n \rightarrow \mathbb{R}^n$. For this system, its initial conditions or initial states are $\xi(t_0)$ where $t_0 \in \mathbb{R}_+$. The time variable t is defined on the interval $[t_0, \infty)$.

The idea of the sliding mode control is highly related with the finite-time stability. This time however often depends on the initial conditions of the system. The case when convergence time is uniform and independent of the initial conditions is known as fixed time stability Cruz-Zavala et al. (2010). Polyakov (2012) gives a precise statement of the fixed time stability :

Definition 2.1. (Globally fixed-time attraction). Let a non-empty set $M \subset \mathbb{R}^n$. It is said to be globally fixed-time attractive for the system (1) if any solution $\xi(t, \xi_0)$ of (1) reaches M in some finite time moment $t = T(\xi_0)$ and the settling-time function $T(\xi_0) : \mathbb{R}^n \rightarrow \mathbb{R}_+ \cup \{0\}$ is bounded by some positive number T_{\max} , i.e. $T(\xi_0) \leq T_{\max}$ for $\xi_0 \in \mathbb{R}^n$.

Note that there are several choices for T_{\max} , for example if $T(x_0) \leq T_m$ for a positive number T_m , also $T(x_0) \leq \lambda T_m$ with $\lambda \geq 1$. This motivates the definition of a set which contains all the bounds of the settling-time function.

Definition 2.2. (Settling-time set). Let the set of all the bounds of the settling-time function for system (1) be defined as follows:

$$\mathcal{T} = \{T_{\max} \in \mathbb{R}_+ : T(x_0) \leq T_{\max}\}. \quad (2)$$

In addition, the minimum bound for the settling-time function of (1) is defined as:

Definition 2.3. (Minimum bound for the settling-time set). Consider the set \mathcal{T} defined in (2), let the time $T_f \in \mathbb{R}$ such that

$$T_f = \{T \in \mathcal{T} : T \leq T_{\max}, \forall T_{\max} \in \mathcal{T}\}. \quad (3)$$

Note that for some systems T_{\max} can be tuned by a particular selection of the system parameters, this notion refers to the prescribed-time stability which is given in Fraguela et al. (2012) and the predefined-time stability Sanchez-Torres et al. (2015). The prescribed-time stability based design and the predefined-time stability based design are explained in the following definitions.

Definition 2.4. (Prescribed-time based design). Consider the set \mathcal{T} defined in (2). The particular case when for the system (1), T_{\max} can be tuned by a particular selection of the system parameters ρ , $T_{\max} = T_{\max}(\rho)$, is referred to the notion of the prescribed-time stability which is given in Fraguela et al. (2012). This design is performed by

selecting $T_{\max}(\rho) \in \mathcal{T}$ and calculating the inverse of the settling-time function, allowing the tuning of ρ .

It is worth to note, the true fixed stabilization time for a system designed based on prescribed-time stability is unknown but bounded by $T_{\max}(\rho)$. In contrast, a designed system with predefined-time stability has a known stabilization time.

Definition 2.5. (Predefined-time based design). The particular case when for the system (1), the time T_f defined in (3) can be tuned by a particular selection of the system parameters ρ , $T_f = T_f(\rho)$, is referred to the notion of the predefined-time stability.

With the definition of a predefined-time attractive set, the following lemma provides a Lyapunov characterization of a class of these sets on the state space:

Lemma 2.1. (Lyapunov function Sanchez-Torres et al. (2015)). If there exists a continuous radially unbounded function

$$V : \mathbb{R}^n \rightarrow \mathbb{R}_+ \cup \{0\}$$

such that $V(x) = 0$ for $x \in M$ and any solution $x(t)$ satisfies

$$\dot{V} \leq -\frac{\alpha}{p} \exp(V^p) V^{1-p} \quad (4)$$

for $\alpha > 0$ and $0 < p \leq 1$, then the set M is globally predefined-time attractive for the system (1) and $T_{\max} = \frac{1}{\alpha} + t_0$.

Proof See Sanchez-Torres et al. (2015).

Definition 2.6. (Predefined-time stabilizing function). For $x \in \mathbb{R}^n$, the predefined-time stabilizing function is defined as

$$\Phi_p(x) = \frac{1}{p} \exp(\|x\|^p) \frac{x}{\|x\|^p} \quad (5)$$

where $0 < p \leq 1$.

With the definition of the stabilizing function, let the following dynamic system:

Lemma 2.2. (Predefined-time stable dynamical system). For every initial condition x_0 , the system

$$\dot{x} = -\frac{1}{T_c} \Phi_p(x) \quad (6)$$

with $T_c > 0$, and $0 < p \leq 1$ is predefined-time stable with settling-time T_c . That is, $x(t) = 0$ for $t > t_0 + T_c$ in spite of the x_0 value.

Proof See Sanchez-Torres et al. (2015).

In order to apply the previous result to control design, consider the dynamic system

$$\dot{\xi} = \Delta(\xi, t) + u \quad (7)$$

with $\xi, u \in \mathbb{R}^n$ and $\Delta : \mathbb{R}_+ \times \mathbb{R}^n \rightarrow \mathbb{R}^n$. The main objective is to drive the system (7) to the point $\xi = 0$ in a predefined fixed time in spite of the unknown non-vanishing disturbance $\Delta(\xi, t)$. A solution to this problem which does not require an individual selection of each of the n control variables based on the *unit control* is presented in the following theorem:

Theorem 2.1. (Predefined-time multivariable control). Let the function $\phi(\xi, t)$ to be bounded as $\|\Delta(\xi, t)\| \leq \delta$, with $0 < \delta < \infty$ a known constant. Then, by selecting the control input

$$u = - \left(\frac{1}{T_c} + \delta \right) \frac{\xi}{\|\xi\|} \exp(\|\xi\|)$$

with T_c being a scalar, the system (7) is globally predefined-time stable with settling-time upper bounded by T_c .

Proof: See Sanchez-Torres et al. (2015).

2.1 Linear Programming Problem Statement

Let the following linear programming problem:

$$\begin{cases} \min_x & \mathbf{c}^T x \\ \text{s.t.} & \mathbf{A}x = \mathbf{b} \\ & l \leq x \leq h \end{cases} \quad (8)$$

where $x = [x_1 \dots x_n]^T \in \mathbb{R}^n$ are the decision variables, $\mathbf{c} \in \mathbb{R}^n$ is a cost vector, \mathbf{A} is an $m \times n$ matrix such that $\text{rank}(\mathbf{A}) = m$ and $m \leq n$; \mathbf{b} is a vector in \mathbb{R}^m and, $l = [l_1 \dots l_n]$, $h = [h_1 \dots h_n] \in \mathbb{R}^n$.

Let $y = [y_1 \dots y_m]^T \in \mathbb{R}^m$ and $z = [z_1 \dots z_n]^T \in \mathbb{R}^n$. Hence, the Lagrangian of (8) is

$$L(x, y, z) = \mathbf{c}^T x + z^T x + y^T (\mathbf{A}x - \mathbf{b}). \quad (9)$$

The KKT conditions establish that x^* is a solution for (8) if and only if x^* , y and z in (8)-(9) are such that

$$\nabla_x L(x^*, y, z) = \mathbf{c} + z + \mathbf{A}^T y = 0 \quad (10)$$

$$\mathbf{A}x^* - \mathbf{b} = 0 \quad (11)$$

$$z_i x_i^* = 0 \text{ if } l_i < x_i^* < h_i, \forall i = 1, \dots, n. \quad (12)$$

3. A RECURRENT NEURAL NETWORK (RNN) FOR LINEAR PROGRAMMING PROBLEM

Following the KKT approach, from Loza-Lopez et al. (2015) a recurrent neural network which solves the problem (8) in finite time is proposed. For this purpose, let $\Omega_e = \{x \in \mathbb{R}^n : \mathbf{A}x - \mathbf{b} = 0\}$ and $\Omega_d = \{x \in \mathbb{R}^n : l \leq x \leq h\}$. According to (8), $x^* \in \Omega$ where $\Omega = \Omega_d \cap \Omega_e$.

From (10), let

$$\dot{x} = -\mathbf{c} + \mathbf{A}^T y + z, \quad (13)$$

then, y and z must be designed such that Ω is an attractive set, fulfilling conditions (10)-(12). For this case, in addition to condition (12), z is considered such that

$$\begin{cases} z_i \geq 0 & \text{if } x_i \geq h_i \\ z_i \leq 0 & \text{if } x_i \leq l_i \end{cases}, \quad (14)$$

and the variable $\sigma \in \mathbb{R}^m$ is defined as

$$\sigma = \mathbf{A}x - \mathbf{b}. \quad (15)$$

In order to obtain predefined-time stability to the solution x^* , the terms y and z are proposed in (13) as

$$y = (\mathbf{A}\mathbf{A}^T)^{-1} \left[\mathbf{A}\mathbf{c} - \mathbf{A}z + \frac{1}{T_s} \phi(\sigma) \right] \quad (16)$$

and

$$z = \left(\|\mathbf{c}\| + \frac{1}{T_s} \right) \varphi(x, l, h) \quad (17)$$

respectively, where $T_s > 0$.

For this case, the multivariable activation functions are $\varphi(x, l, h) = [\varphi_1(x, l_1, h_1) \dots \varphi_n(x, l_n, h_n)]^T$, with $\varphi_i(x, l_i, h_i)$ of the form

$$\varphi_i(x, l_i, h_i) = \begin{cases} -\frac{x_i - l_i}{\|x - l\|} \exp(\|x - l\|) & \text{if } x_i \leq l_i \\ 0 & \text{if } l_i < x_i < h_i \\ -\frac{x_i - h_i}{\|x - h\|} \exp(\|x - h\|) & \text{if } x_i \geq h_i \end{cases} \quad (18)$$

and

$$\phi(\sigma) = -\frac{\sigma}{\|\sigma\|} \exp(\|\sigma\|). \quad (19)$$

Therefore, with the structure given by (13) and the KKT multiplier as in (16) and (17), with activation functions (18) and (19), the following theorem presents a RNN which solves (8) in predefined-time.

Theorem 3.1. (Predefined-time RNN for linear programming). For the RNN

$$\dot{x} = -\mathbf{c}\Lambda + \left(\|\mathbf{c}\| + \frac{1}{T_s} \right) \Lambda \varphi(x, l, h) + \frac{1}{T_s} \mathbf{A}^+ \phi(\sigma) \quad (20)$$

where $\Lambda = I - \mathbf{A}^T(\mathbf{A}\mathbf{A}^T)^{-1}\mathbf{A}$, $\mathbf{A}^+ = \mathbf{A}^T(\mathbf{A}\mathbf{A}^T)^{-1}$ and $T_s > 0$, the point x^* is globally predefined-time stable with settling-time T_s .

Proof: The dynamics of (15) is given by

$$\dot{\sigma} = \mathbf{A}(-\mathbf{c} + \mathbf{A}^T y + z). \quad (21)$$

Therefore, with the selection of y as in (16), the system (21) reduces to

$$\dot{\sigma} = -\frac{1}{T_s} \frac{\sigma}{\|\sigma\|} \exp(\|\sigma\|).$$

Thus, from *Theorem 2.1*, a sliding mode is induced on the manifold $\sigma = 0$. Therefore, the set Ω_e is predefined-time attractive with settling-time T_s .

On the manifold $\sigma = 0$, the equivalent value of ϕ is the solution of $\dot{\sigma} = 0$. Resulting to $\phi_{\text{eq}} = 0$ or $y_{\text{eq}} = (\mathbf{A}\mathbf{A}^T)^{-1}[\mathbf{A}\mathbf{c} - \mathbf{A}z]$. Therefore, the dynamics of (13) on that manifold is

$$\dot{x} = -\mathbf{c}\Lambda + \Lambda z. \quad (22)$$

With the selection of z as in (17), the resulting system (22) is

$$\dot{x} = -\mathbf{c}\Lambda + \Lambda \left(\|\mathbf{c}\| + \frac{1}{T_s} \right) \varphi(x, l, h).$$

Consider the Lyapunov function $V = \|x\|$. Its derivative is given by $\dot{V} = \frac{x^T}{\|x\|} \dot{x}$. Therefore

$$\begin{aligned} \dot{V} &= \frac{x^T}{\|x\|} \left[-\mathbf{c}\Lambda + \Lambda \left(\|\mathbf{c}\| + \frac{1}{T_s} \right) \varphi(x, l, h) \right] \\ &\leq \frac{x^T}{\|x\|} \left[\frac{1}{T_s} \varphi(x, l, h) \right]. \end{aligned} \quad (23)$$

Replacing the Lyapunov function

$$\dot{V} \begin{cases} \leq -\frac{1}{T_s} \exp(V) & \text{if } x < l \text{ or } x > h \\ = 0 & \text{if } l \leq x \leq h \end{cases} \quad (24)$$

From *Theorem 2.1*, the set Ω_d is predefined-time attractive with settling-time T_s .

In the set Ω_d the equivalent value of φ , φ_{eq} , is the solution to $\dot{x} = 0$. With the application of *Theorem 2.1*, the conditions (11) and (12) are satisfied, providing predefined-time convergence to the set Ω . Now, by using the equivalent control method, the solution of $\dot{x} = 0$ and $\dot{\sigma} = 0$ in (13) for $t > T_s$ has the form

$$\mathbf{c} + \mathbf{A}^T y_{eq} + z_{eq} = 0.$$

Therefore, the condition (10) is fulfilled, implying the point $x^* \in \Omega$ is globally predefined-time stable. ■

Remark 3.1. Note that, in contrast to the most of the RNN presented in the literature, this scheme only needs the tuning of one variable, namely T_s in spite of the problem dimensions.

4. OPTIMIZATION OF THE POWER DISPATCH IN A MICROGRID SIMULATION

The optimization algorithm previously presented is applied to the power dispatch problem within a simulated microgrid in order to minimize the consumption of power provided by the utility grid.

4.1 Microgrid Description

The simulated microgrid is connected as in Loza-Lopez et al. (2014), with a *wind power system* (WPS), a connection point with the *utility grid system* (UGS) and a DC voltage bus, which includes the output load, a *solar power system* (SPS), and a *battery bank system* (BBS).

The microgrid simulation is performed in Simulink with the Simscape Power Systems¹ libraries, which include the dynamic simulation of electronic components in order to produce a better approach to a real electrical microgrid. Discrete sliding modes controllers are applied to solar, battery bank and wind power systems.

Wind Power System. The connection and control of the WPS is as in Ruiz et al. (2011) which includes a doubly fed induction generator (DFIG) with a mechanical interconnection to a wind turbine. The DFIG stator is directly connected to the utility grid while the rotor is coupled by a back to back converter. This connection scheme requires two different controllers; one is the grid side controller (GSC), which is in charge of maintaining a fixed voltage in the capacitor, and the second one is the rotor side controller (RSC), which controls the electrical torque T_e according to the mechanical torque T_m in the connection with the wind turbine. Both of these controllers maintain a desired power factor of the energy delivered to the grid.

In Rapheal et al. (2009) the maximum mechanical power for a wind turbine is directly related to a constant value of its tip speed ratio λ :

$$\lambda = \frac{\omega_t R_t}{v}$$

where ω_t is the turbine rotor angular speed in rad/s, v is the wind speed m/s and R_t is the wind turbine rotor

¹ Simulink/Simscape Power Systems are trademarks of The MathWorks, Inc.

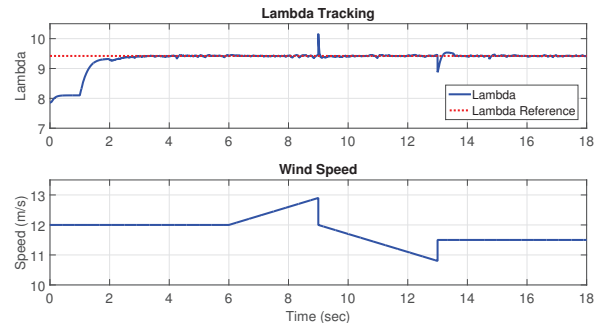


Figure 1. WPS lambda tracking under wind speed variations.

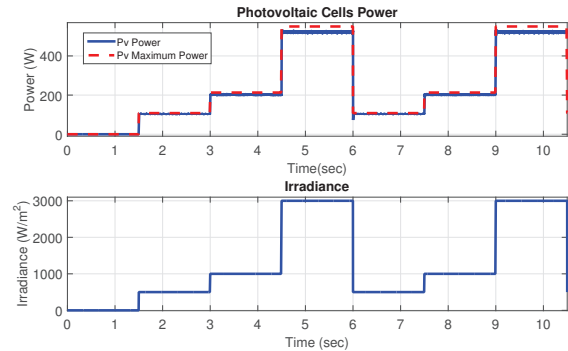


Figure 2. SPS maximum power tracking under irradiance variations.

radius (m). In order to produce the maximum power from the WPS under wind speed variations, λ needs to be transformed to an electrical torque (Ruiz et al. (2011)) and be passed as the reference to track by the RSC. In Fig. 1, the performance under wind speed variations of the WPS can be observed, in this case the λ reference to track corresponds to the maximum power point given by the wind turbine block in Simulink.

Solar Power System. The SPS is simulated by a 213 W Simscape Power Systems block with a maximum power point tracker (MPPT) control system, which includes a *perturb and observe* algorithm (de Brito et al. (2013)) to obtain the photovoltaic panel voltage that corresponds to the maximum power $V_{pv,max}$, and a DC-DC buck converter in order to track this voltage.

The DC-DC buck converter is directly connected to the output of the SPS as in Koutroulis et al. (2001), this allows the $V_{pv,max}$ tracking without the problem of high voltage in the output of the converter. A discrete equivalent control is applied to the insulated-gate bipolar transistor (IGBT) of the DC-DC converter with a pulse width modulation (PWM) block interface. The IGBT switching produces noise in the required measurements for the control system as it would in real time application. In Fig 2, the performance of the SPS along with the MPPT control system under irradiance variations is displayed, the blue line corresponds to the maximum power obtained by the buck converter with the perturb and observe algorithm, and the red dot line is the maximum theoretical power in the photovoltaic panel.

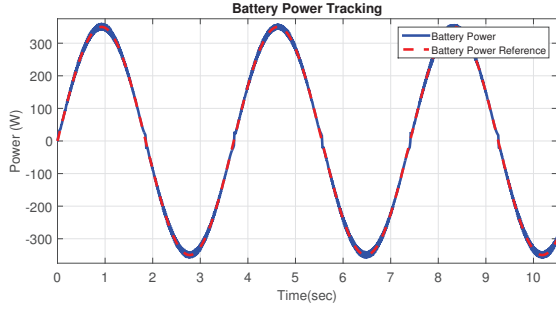


Figure 3. Battery power and reference.

Battery Bank System. The BBS is simulated by a lead-acid 24 V, 100 Ah battery Simulink block. The control system for this BBS is implemented using a parallel buck and boost DC-DC converters; the first one is used under discharge conditions and the second one under charge conditions. A discrete equivalent controller is applied to the each converter, and they switch according to the sign of the reference power to track. In Fig 3, the performance of these controllers acting together is displayed. The blue line is the power given or extracted by the BBS, and the red dot line is a sinusoidal power reference to track.

4.2 Microgrid Optimization Approach

The main goal for this test is to optimize the power dispatch of the microgrid based on the output power of the load at time k (P_{Lk}).

The optimization problem is expressed as follows:

$$\left\{ \begin{array}{l} \text{Minimize} \quad 10P_{Gk} - 500P_{Wk} - 500P_{S_k} - 200P_{B_k} \\ \text{s.t.} \quad P_{Gk} + P_{Wk} + P_{S_k} + P_{B_k} = P_{Lk} \\ P_{G_{min}} \leq P_{Gk} \leq P_{G_{max}} \\ P_{W_{min}} \leq P_{Wk} \leq P_{W_{max}} \\ P_{S_{min}} \leq P_{S_k} \leq P_{S_{max}} \\ P_{B_{min}} \leq P_{B_k} \leq P_{B_{max}} \end{array} \right. \quad (25)$$

In order to match the form of the equation (8), the needed matrices are established as: $\mathbf{c}^T = [10 \ -500 \ -500 \ -200]^T$, $\mathbf{x} = [P_{Gk} \ P_{Wk} \ P_{S_k} \ P_{B_k}]^T$, $\mathbf{A} = [1 \ 1 \ 1 \ 1]$, $\mathbf{b} = [P_{Lk}]$, $\mathbf{l} = [P_{G_{min}} \ P_{W_{min}} \ P_{S_{min}} \ P_{B_{min}}]$ and $\mathbf{h} = [P_{G_{max}} \ P_{W_{max}} \ P_{S_{max}} \ P_{B_{max}}]$. Where P_{Gk} , P_{Wk} , P_{S_k} and P_{B_k} are the UGS, WPS, SPS and BBS powers at time k , and the matrices \mathbf{l} and \mathbf{h} are their corresponding minimum and maximum power values according to the wind speed in the WPS, the temperature and irradiance in the SPS and the state of charge of the BBS.

4.3 Simulation Results

The presented optimization method uses the measured load power as the vector \mathbf{b} and the matrices defined in the previous section to set the references of power for the microgrid. Due to incentivize the use of the available power given by the SPS, WPS and BBS, the expectation is that the power references for these three systems are set near to their maximum power limits. For this test the settling time T_c is set to $5e^{-5}$ sec to guarantee an appropriate reference

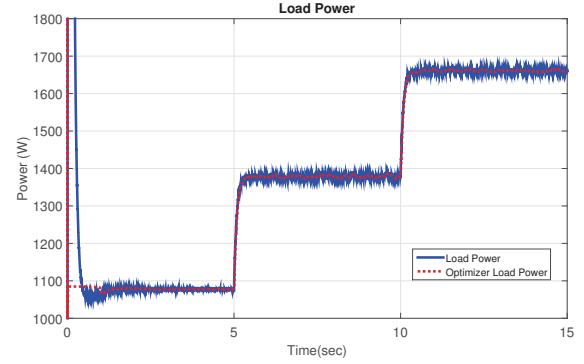


Figure 4. Load power and references sum

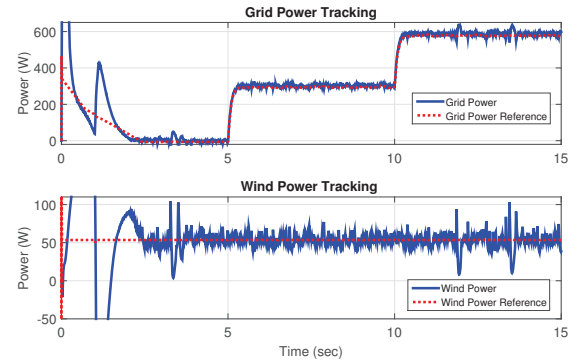


Figure 5. UGS and WPS power tracking

tracking, the wind speed is set to 12 m/s which correspond to a $P_{W_{min}}$ and $P_{W_{max}}$ of 0 and 53.5 W. The temperature and irradiance in the photovoltaic panel are set to 25 °C and 3000 W/m² with a $P_{S_{min}}$ and $P_{S_{max}}$ of 0 and 530 W. The state of charge of the battery is 50% which is a neutral state with a discharging and charging maximum powers of -500 and 500 W respectively. Even though the UGS is simulated by an infinite bus, in this test the $P_{G_{min}}$, and $P_{G_{max}}$ are fixed to -1000 and 1000 W. Three different loads are implemented, at the beginning a 0.13 Ω resistor is connected to the DC voltage bus, at 5 seconds a 0.5 Ω is added in parallel and at 10 seconds another 0.5 Ω is connected in the same way.

In Fig 4, the red dot line represents the sum of all the power references given by the optimization method, and the blue line is the measured load power. It can be seen that the equality restriction given in (25) is respected.

In Fig. 5, the UGS and the WPS power dynamics are shown. It can be seen that wind power reference is near to the maximum power limit as expected to the related cost fixed in (25). In the UGS power dynamics it can be seen that when the WPS, BBS and SPS powers are not enough to supply the power of the load, the remaining power is delivered through the UGS. This condition occurs particularly when the two 5 Ω parallel resistors are added to the DC bus in 5 and 10 seconds.

In Fig. 6, the blue lines represent the SPS and BBS power and the red dot lines are the optimal power references. It can be seen that the limits established in (25) for these two systems and the reference tracking are fulfilled. The SPS

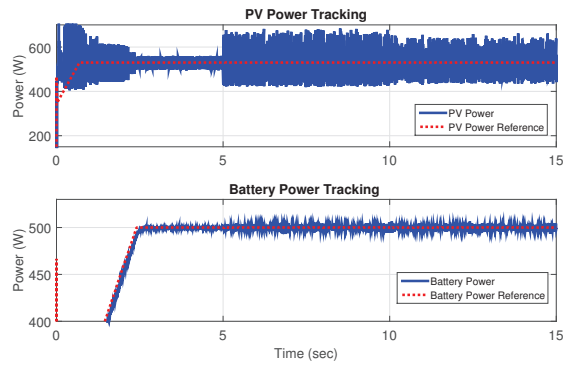


Figure 6. SPS and BBS power tracking.

power reference remains almost all the simulation in the maximum value allowed for this system, this is because of the previously fixed cost related to this system.

5. CONCLUSION

In this paper the optimal power dispatch within a microgrid is found. The microgrid consists of a connection point with the utility grid, a battery bank system, a solar panel system and a wind power system, with appropriate control systems for the last three. A novel recurrent neural network which solves linear programming problem, provides the references to be followed by each controller. The main features of the proposed neural network are predefined convergence time and the tuning of only one parameter. The simulation results validate the use of the presented optimization algorithm. In all simulations, the component dynamics with real parameters were taken into account, which provide a feasible framework for future real-time implementation.

REFERENCES

Aquino, R., Carvalho, M., Neto, O., Lira, M.M.S., de Almeida, G., and Tiburcio, S. (2010). Recurrent neural networks solving a real large scale mid-term scheduling for power plants. In *Neural Networks (IJCNN), The 2010 International Joint Conference on*, 1–6.

Chowdhury, S. and Crossley, P. (2009). *Microgrids and Active Distribution Networks*. IET renewable energy series. Institution of Engineering and Technology.

Cichocki, A. and Unbehauen, R. (1993). *Neural networks for optimization and signal processing*. J. Wiley.

Cruz-Zavala, E., Moreno, J., and Fridman, L. (2010). Uniform second-order sliding mode observer for mechanical systems. In *Variable Structure Systems (VSS), 2010 11th International Workshop on*, 14–19.

de Brito, M.A.G., Galotto, L., Sampaio, L.P., d. A. e Melo, G., and Canesin, C.A. (2013). Evaluation of the main mppt techniques for photovoltaic applications. *IEEE Transactions on Industrial Electronics*, 60(3), 1156–1167.

Fraguela, L., Angulo, M., Moreno, J., and Fridman, L. (2012). Design of a prescribed convergence time uniform robust exact observer in the presence of measurement noise. In *Decision and Control (CDC), 2012 IEEE 51st Annual Conference on*, 6615–6620.

Karush, W. (1939). *Minima of functions of several variables with inequalities as side constraints*. Master's thesis, Dept. of Mathematics, Univ. of Chicago, Chicago, Illinois.

Korovin, S.K. and Utkin, V.I. (1974). Using sliding modes in static optimization and nonlinear programming. *Automatica*, 10(5), 525–532.

Koutroulis, E., Kalaitzakis, K., and Voulgaris, N.C. (2001). Development of a microcontroller-based, photovoltaic maximum power point tracking control system. *IEEE Transactions on Power Electronics*, 16(1), 46–54. doi:10.1109/63.903988.

Kuhn, H.W. and Tucker, A.W. (1951). Nonlinear programming. In *Proc. Second Berkeley Symp. on Math. Statist. and Prob. (Univ. of Calif. Press)*.

Loza-Lopez, M.J., Loukianov, A.G., Sanchez, E.N., Ruiz-Cruz, R., and Sanchez-Torres, J.D. (2015). On-line optimization of the power supplied in a microgrid prototype. In *Smart Cities Conference (ISC2), 2015 IEEE First International*, 1–6.

Loza-Lopez, M.J., Sanchez, E.N., and Ruiz-Cruz, R. (2014). Microgrid laboratory prototype. In *Power Systems Conference (PSC), 2014 Clemson University*, 1–5. doi:10.1109/PSC.2014.6808120.

Pazos, F.A. and Bhaya, A. (2009). Control Liapunov function design of neural networks that solve convex optimization and variational inequality problems. *Neurocomputing*, 72(1618), 3863–3872.

Polyakov, A. (2012). Nonlinear feedback design for fixed-time stabilization of linear control systems. *IEEE Transactions on Automatic Control*, 57(8), 2106–2110.

Pyne, I.B. (1956). Linear programming on an electronic analogue computer. *American Institute of Electrical Engineers, Part I: Communication and Electronics, Transactions of the*, 75(2), 139–143.

Rapheal, M.S.A., Ram, V.G., Ramachandaramurthy, V.K., and Hew, W.P. (2009). Dynamic response of different wind generator topologies connected to medium size power grid. In *PowerTech, 2009 IEEE Bucharest*, 1–6.

Ruiz, R., Sanchez, E.N., Loukianov, A.G., and Harley, R.G. (2011). Discrete-time block control for a doubly fed induction generator coupled to a wind turbine. In *Proceedings of the IEEE International Conference on Control Applications (CCA)*. Denver, CO, USA.

Sanchez-Torres, J., Sanchez, E., and Loukianov, A. (2015). Predefined-time stability of dynamical systems with sliding modes. In *American Control Conference (ACC), 2015*, 5842–5846.

Utkin, V. (1992). *Sliding modes in control and optimization*. Springer Verlag.

Wang, J. (1993). Analysis and design of a recurrent neural network for linear programming. *IEEE Transactions on Circuits and Systems I: Fundamental Theory and Applications*, 40(9), 613–618.

Wilson, G. (1986). Quadratic programming analogs. *IEEE Transactions on Circuits and Systems*, 33(9), 907–911.